ATLAS Internal Note
INDET-NO-xxx
January 13, 2000

Studies of wire offset effects on gas gain in the ATLAS TRT straw chamber

P. Cwetanski[a], A. Romaniouk[a], V. Sosnovtsev[b]

[a] *CERN, Geneva, Switzerland*
[b] *Moscow Engineering and Physics Institute, Moscow, Russia* Germany

Abstract

Results of measurements and simulation (both analytical and Monte Carlo) of the amplification process in straw tubes used in the ATLAS Transition Radiation Tracker are presented. Main attention was paid to studies of the evolution of the signal amplitude spectrum for a point ionization as a function of the wire offset in the TRT standard gas mixture. The agreement between experimental data and simulation shows that the understanding of the intrinsic behavior of the detector is good. This provides not only explanation of processes in the straw but a solid basis for the choise of the gas mixture for the wire offset measurement in the ATLAS TRT as well.

1 Introduction

The straw tube Transition Radiation Tracker (TRT) in the ATLAS experiment [1] at LHC is being designed to operate at extremely high radiation levels. Some elements of the 425,000 straw proportional tube detector are expected to operate at rates approaching 20 MHz and even these straws should provide reliable tracking and particle identification information.

The straw geometry, the exact gas composition, straw voltage and gas gain are only a few of many parameters that play an important role in defining the detector performance.

The standard TRT gas mixture $Xe/CF_4/CO_2$ 70/20/10 provides an efficient X-ray absorption, a fast charge collection and a stable operation over a sufficient high-voltage range even at high particle rates. However the large fraction of carbon tetrafluoride (CF_4), well known as a "fast gas" with very good ageing performance, leads to electronegative properties of the gas mixture in high electric fields and therefore causes capture of electrons drifting towards the anode wire [2, 3] what affects the energy resolution of the straw chamber.

The electron amplification near the anode wire is the main process, contributing to the straw signal. It strongly depends on the electric field and chamber geometry. A displacement of the anode wire from the straw tube center (wire offset) distorts the radial symmetry of the electric field (Section 3.3) and leads to a change of the amplitude spectrum of the straw. Experimental studies performed with straws have shown that wire offsets smaller than 300 μm do not essentially deteriorate the detector performance [1]. Nevertheless their effects on the signal amplitude distribution are not negligible and this fact is used as a technique for wire offset measurements for all 425,000 straws of the assembled ATLAS TRT [1]. That is the main motivation for studies of the impact of wire offsets on electron multiplication and energy resolution of the straw chamber. The main part of this work was dedicated to this issue, examined in various measurements and then compared with analytic simulations and Monte Carlo studies. Different gas mixtures and recommendations for wire offset measurements in the ATLAS TRT are discussed as well.

2 Measurements

A schematic view of the experimental setup is shown in Fig. 1.

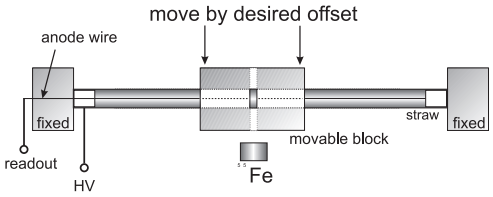

Figure 1: *Experimental setup for the wire offset measurements (parallel wire offset).*

While the 12 cm long straw was fixed at its ends a parallel wire offset was realized by enforcing the middle part (of about 1 cm) of the straw into a polycarbonate block that could be shifted perpendicular to the wire axis. This method ensured always a parallel position of the tube with respect to the wire in the irradiated part. The straw could be irradiated through 1 mm wide collimating slits either from the side where the wire is closest to the tube wall, from the opposite side or from a position which is perpendicular to

the plane of the straw movement. Several spectra of an ^{55}Fe source, emitting 5.95 keV X-rays, have been recorded in order to measure gas gain and energy resolution with respect to different wire offsets. The anode wires had diameters of 30 μm and of 50 μm with tolerance better than 1%. TRT standard Xenon gas mixture and several Argon based mixtures containing CO_2 and CF_4 were examined.

The multiplication factor and energy resolution were determined from recorded ^{55}Fe spectra for various anode voltages and wire offsets by reading out the position of the peak (corresponds to most probable gain) and its FWHM (full width half maximum).

At the very beginning, dedicated studies were performed to examine the effects which can appear when the wire does not have a parallel offset but it is positioned with some angle to the straw axis. In the set-up for the measurements with angular wire displacement the wire had central position at one end of the straw, whereas at the other end it was crimped outside of the 1.5 mm thick wire crimping pin and therefore displaced by 750 μm.

Changing collimated source positions data with any offset between 0 and 750 μm could be sampled. It turned out, that there is no measurable difference in behavior between parallel and angular (with respect to the straw axis) wire displacement.

The results of peak position measurements as a function of wire offset for 30 μm wire and the standard Xenon gas mixture are shown in Fig. 2. The three sets of data shown there correspond to different directions of the X-ray beam:

Far - straw is irradiated from the side where the wire has the largest distance from the cathode.
Near - straw is irradiated from the side where the wire has the shortest distance from the cathode.
Up - straw is irradiated from the side perpendicular to the wire displacement plane.

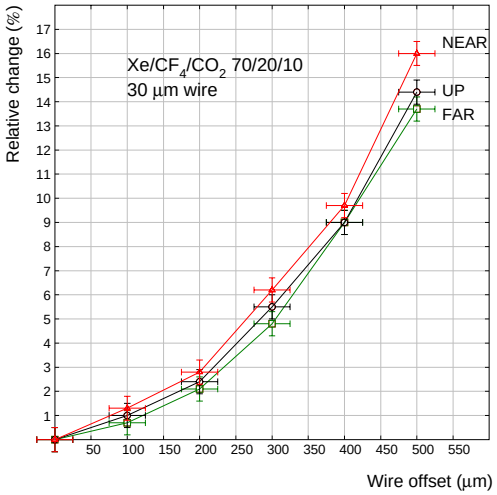

Figure 2: *Gas gain change as a function of the anode wire displacement for different directions of X-ray beam. TRT standard mixture, 30 μm wire diameter.*

In case of uniform X-ray absorption in the straw there would be no measurable difference when changing the direction of irradiation (direction **Up** represents this case). However in reality the attenuation length for 6 keV photons in Xenon is about 2 mm, which creates an asymmetry in absorbed photon density in the straw. The signal amplitude therefore results from the azimuthal position of the electrons drifting towards the displaced wire.

Additional experimental data on wire offset effects can be found in Section 4 and in the Appendix.

3 Simulations

3.1 Software

The following software was used to investigate the described subject:

Garfield [4] - a computer program for the detailed simulation of two- and three-dimensional drift chambers which includes drifting of particles, diffusion, avalanching and current induction.

Magboltz [5] - computes transport properties for electrons in various gases, including drift velocity, the longitudinal and transverse diffusion coefficients and the Townsend and attachment coefficients. A large set of the latest cross-sectional data for numerous gases is included in the code.
The program is available either in the traditional version performing a multiterm Boltzmann analysis (program simply called *"Magboltz"*) or a new version using Monte Carlo methods to compute the described quantities (unofficial program name *"mmonte"*). Of the latter also exists a refined version (unofficial program name *"imonte"*) [1] for higher accuracy computation of the Townsend and attachment coefficient in high field regions (E < 50 kV/ cm). It is strongly recommended to use this Monte Carlo programs for simulation in magnetic fields. High accuracy in simulations is achieved by tracking all electrons created in ionizing collisions. The Boltzmann transport equation solved in the analytic version of Magboltz uses a solution for the energy distribution function expanded up to the third term of the Legendre polynomials [6]. It should be mentioned that for the drift velocity calculation in the Xenon standard mixture the Boltzmann code of Magboltz was slightly modified for better agreement. The electron energy upper integration limit was limited to values where the electron energy distribution function, F0, was greater than 10^{-6} eV, this helped to improve the numerical accuracy of the calculation [7].

[1] all Monte Carlo versions available from Steve Biagi

3.2 Gas properties

In order to simulate the straw operation the following transport properties of electrons in the standard ATLAS TRT gas mixture $Xe/CF_4/CO_2$ 70/20/10 had to be determined: drift velocity, both transversal and longitudinal diffusion, ionization and attachment coefficients.

A comparison with the available experimental data served as a first benchmark for the reliability of the simulation with the different versions of Magboltz. As mentioned before the electron drift velocity (Fig. 3) (for E < 10 kV/cm) was found to agree much better with the experimental data using the modified analytic Boltzmann version of Magboltz with its modified truncation of the electron energy distribution function F0. However calculating the diffusion (Fig. 4), ionization and attachment coefficients (Fig. 5) is proven to be more accurate using the Monte Carlo integrator [6]. The technique has been previously described by Fraser and Mathieson [8] and will not be discussed here.

It is interesting to note focussing effect of the electric field in the straw which compensate transverse diffusion effects. Fig. 6 and Fig. 7 show simulated tracks of of single electrons drifting from three position inside of the straw. One can see that final size of the electron cloud drifting from point

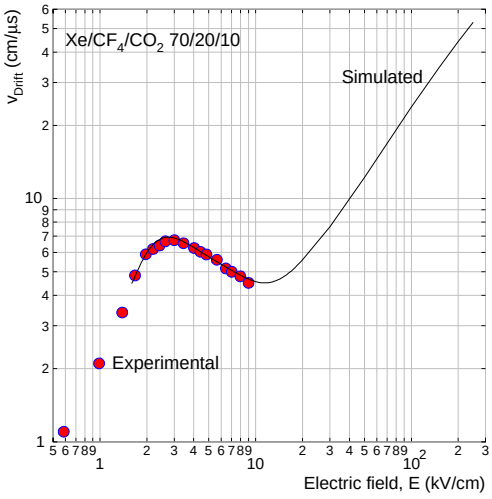

Figure 3: *Computed and measured electron drift velocity in the TRT standard mixture. Experimental data taken from Ref. [1].*

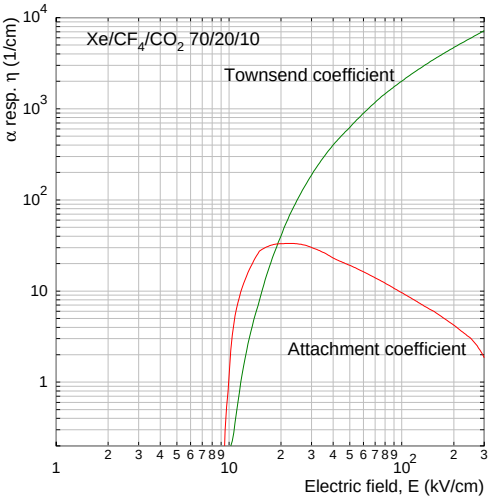

Figure 5: *Calculated Townsend and attachment coefficient in the TRT standard mixture.*

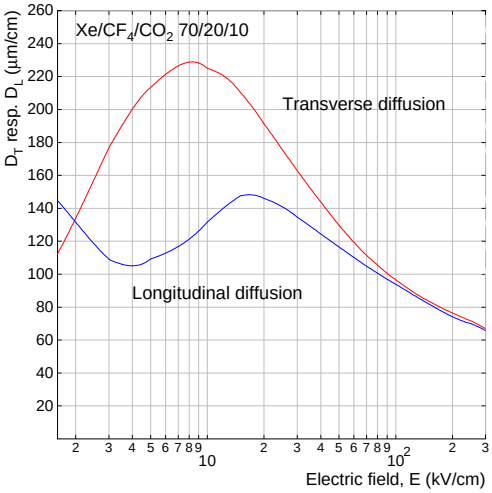

Figure 4: *Simulated transverse and longitudinal diffusion coefficients in the TRT standard mixture.*

ionozation occupies only 15 % of the straw surface.

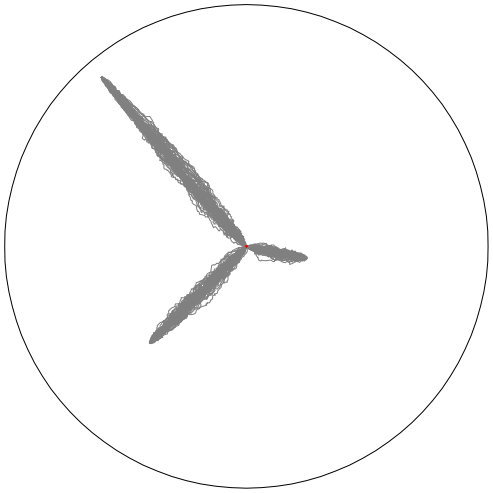

Figure 6: *Drift of randomly placed point-like ^{55}Fe clusters in the TRT straw. Note the focussing effect.*

3.3 Electric field in the straw

The modeling of the straw tube geometry could be easily done in two dimensions, i. e. only the cross-section of the straw has been drawn and sym-

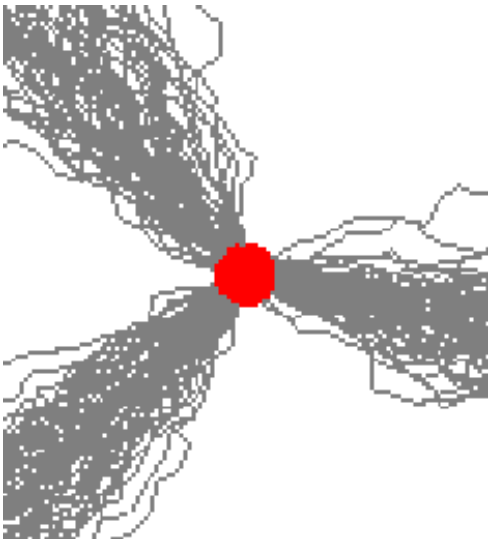

Figure 7: *The zoomed view clearly shows the focussed drift towards the wire.*

metry along the tube axis assumed in order to simplify the calculations.

The tube with an inner diameter of 4 mm was assumed to be perfectly round, since small deviations towards an elliptical shape have a negligible effect on the electric field and can be kept out of examination. Garfield allows an easy description of the geometry in two dimensions and calculates the field inside the straw analytically following the known relation for the electric field in a cylindrical geometry:

$$E(r) = \frac{V}{r \cdot \log(\frac{b}{a})}$$

V = *voltage applied between anode and cathode*
a = *anode wire radius*
b = *cathode inner radius*

The field map for configurations with a displaced wire is obtained through a conformal mapping of the solution for the centered wire and exact in the thin wire limit. Field line plots for 500 μm wire offset can be seen in Fig. 8 and Fig. 9. In addition an attempt was done to examine a finite element analysis (FEM) using the commercial field simulation package *Maxwell* [9]. This would be necessary if we saw 3D effect of the field on the avalanche development for tilted anode wire. It quickly became clear that this is not suitable for our case, because the description of the potential with a second-order function leads only to a linear approximation of the field (which is the derivative) and hence lacks accuracy in the region close to the wire where the avalanch fromation occurs.

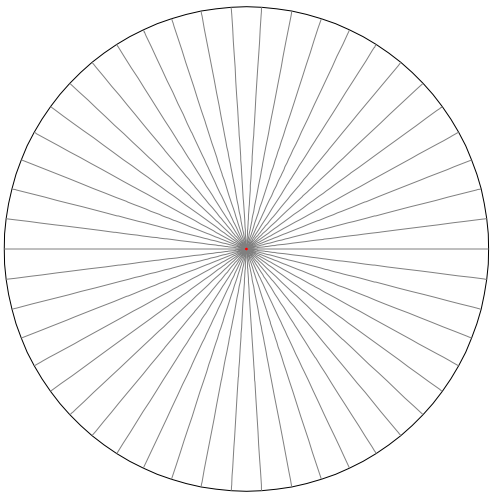

Figure 8: *Field lines in a straw tube with no wire offset.*

It is suggestive to view the electric field at the wire surface, especially its change with increasing wire offset. It was done for anode voltage of 1530 V (TRT operation voltage). The wire was shifted out of the center, which resulted in an enhanced field on the wire surface. The results are shown in Table 1.

The development of the surface field for different wire offsets is shown in Fig. 10 as a function of azimuthal an-

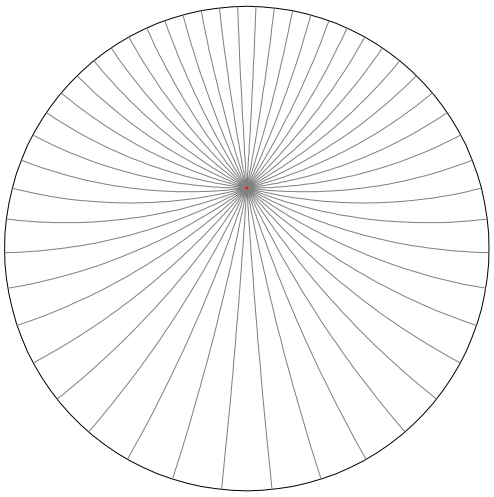

Figure 9: *Field lines in a straw tube with a wire offset of 500 μm.*

offset [μm]	E_{avg} [kV/cm]	E_{min} [kV/cm]	E_{max} [kV/cm]
0	208.47	208.47	208.47
200	208.90	209.07	208.72
300	209.44	209.70	209.17
400	210.22	210.59	209.85
500	211.25	211.72	210.79

offset [μm]	relative change [%]	correspond. voltage [V]
0	0.0	1530
200	0.2	1534
300	0.5	1537
400	0.8	1543
500	1.3	1550

Table 1: *Electric field at wire surface vs. wire offset.*

gle.

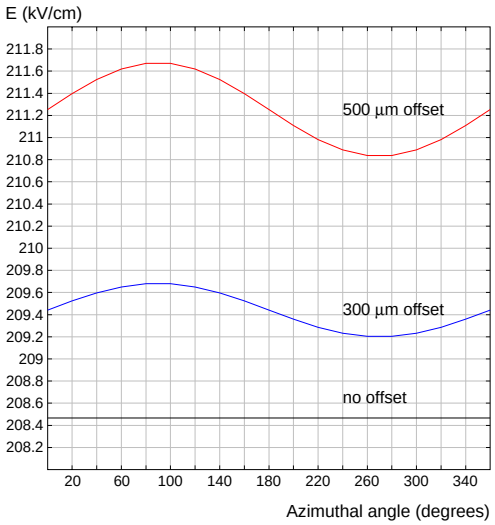

Figure 10: *Electric field strength on the wire surface for no offset, 300 μm and 500 μm offsets. The wire was displaced in the direction of 90 degrees azimuthal angle (point on wire surface closest to the cathode).*

Note that with the wire moving towards the cathode the electric field increases on the whole wire surface. Over all one clearly expects a total increase of the most probable gain with respect to the wire offset and besides a broadening of the spectrum, as the field strength is no longer uniform on the wire surface. Avalanches developing towards the wire from the side closest to the tube will result in larger sizes than avalanches on the opposite side of the wire. This is only true if the avalanche does not develop around the wire. As it was shown for other gas [10], avalanche from piont-like ionisation in TRT straw filled with standard gas do not embrace the wire at the operating gas gain. Fig. 14 shows simulation results for avalanche development near the wire.

3.4 Avalanching model

The statistical distribution of the carrier number of single electron avalanches in a Townsend discharge is described by

$$v(n) = \frac{1}{\bar{n}} \cdot e^{-\frac{n}{\bar{n}}} \quad (1)$$

with

$$\bar{n} = e^{\int \alpha dx} \quad (2)$$

$\bar{n}$ = *mean number of electrons in an avalanche*
α = *Townsend coefficient*

This distribution is only valid in absence of attachment, recombination, space charge effects or strong electric fields. However in our case we have to deal with a non-negligible amount of electronegative molecules in the gas mixture causing electron attachment, hence with the fact that only a part of the primary electrons form observable avalanches. These are still subject to an exponential distribution but with an increased mean except zero bin which correcponds captured electrons. (Fig. 11). A detailed theoretical discussion of this topic was done by W. Legler [11, 12].

The introduction of the attachment coefficient η leads to a more complicated description of the avalanche distribution in non-uniform electric fields since both Townsend and attachment coefficients are subject to fluctuations. The implementation of an independent treatment of Townsend and attachment fluctuations in the code of Garfield could be done [13]. That means after each step in the Monte Carlo integration there is a decision whether an electron ionizes, gets attached or continues drifting. In prior

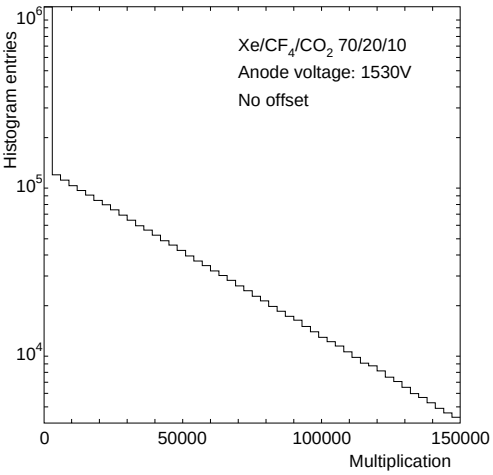

Figure 11: *Number of electrons in single electron avalanches in the $Xe/CF_4/CO_2$ 70/20/10 gas mixture (straw tube with a 30 μm anode wire at 1530 V, no wire offset).*

versions of the code the final multiplication was just multiplied by an integrated attachment probability, which is a good approximation in gases with low attachment. However only the described method can reveal the deteriaoration of energy resolution due to the electronegative CF_4 admixture.

Fig. 12 shows the comparison of the simulated and experimental spectrum of a straw. One can see very good agreement, although the different peak positions reflect the deviation of the measured peak from the simulated one. The escape peak does not appear in the computed spectrum, since this process is not considered in the simulation (for more details see next Section).

3.5 Straw gas gain and energy resolution

Transport properties in our gas mixture were computed with Magboltz where the temperature was set to 23°C and the pressure atmospheric (760 Torr). We can mention here that

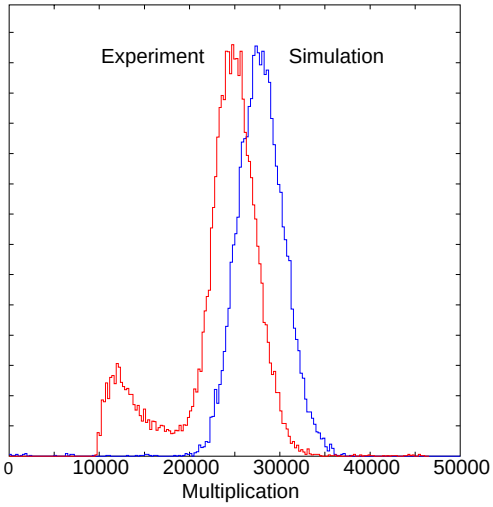

Figure 12: *Comparison of experimental and simulated spectrum of an ^{55} Fe source (gas gain 10% higher).*

the temperature dependence of the gas gain in the experiment has earlier been found to be 1.7% per degree [1].

The average number of primary electrons from an ^{55}Fe conversion including fluctuations was computed by following the avalanching process of a 5.95 keV single electron until all secondary electrons are thermalized [14]. Taking a Fano factor of 0.17 one gets 256 ± 7 electrons per cluster using the known relation for the fluctuations [15]:

$$\sigma_{\mathrm{N}}^2 = \mathrm{F}\bar{\mathrm{N}} \qquad (3)$$

σ_N = *Fluctuations in the number of primary electrons*
F = *Fano factor*
$\bar{\mathrm{N}}$ = *Average number of primary electrons*

In order to obtain the equivalent of an ^{55}Fe spectrum in our simulation the following steps have been done. The average in multiplication of 256 single electron avalanches was computed by drifting all these electrons from the same, randomly chosen position in the straw (diffusion included in the drift process). An example of electron cluster drift (of only 50 electrons per cluster) shown in Fig. 6 and 7.The entirety of some thousand calculated "cluster avalanches", randomly distributed all over the straw, was then plotted into a histogram (Fig. 12) resulting in a peaking distribution from which the most probable value of signal amplitude corresponding to the gas gain value could be determined. A gas gain curve was calculated and compared with the experimental data. It showed agreement within 10% in the region of gain linearity (Fig. 13).

The agreement seen from this figure is remarkable since the total multiplication factor is extremely sensitive on the cross-sectional data of the gas components in the mixture.

For higher multiplication values, commencing space-charge effects in the avalanches lead to a significant nonlinearity in the straw response.

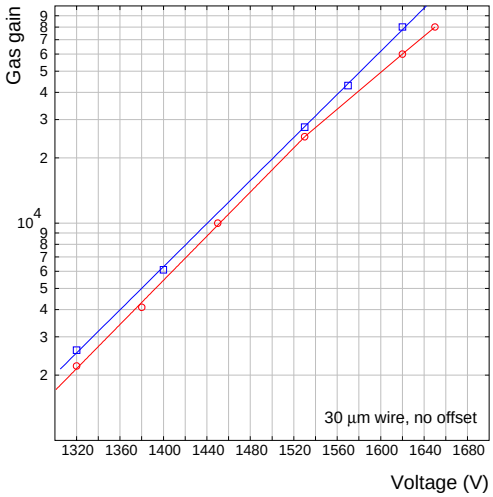

Figure 13: *Gas gain in the TRT standard mixture as a function of voltage. Experimental data and Monte Carlo simulation.*

3.6 Drift processes in the straw

The strong focusing effect of the radial field for the avalanche can clearly be seen in the simulation (Fig. 14). This figure manifest the fact that the avalanches do not embrace the wire and cover only about 25% of azimuthal space. However the electrostatic repulsion in the avalanche is not considered in the simulation. The electron multiplication threshold depends on the gas and lies for the TRT standard mixture at about 30 kV/cm which corresponds to a distance of approximately six wire radii or 90 μm from the wire surface (30 μm wire at 1530 V).

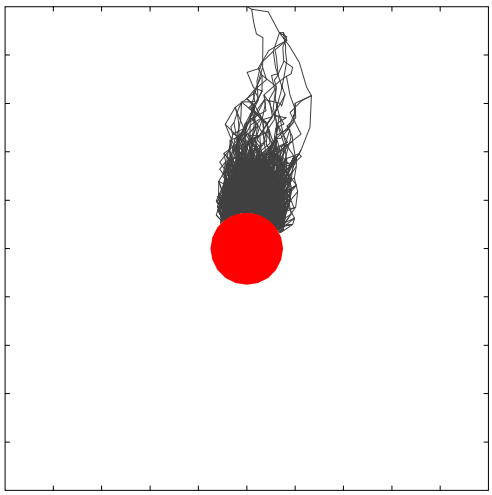

Figure 14: *Single electron avalanche in a straw tube. Gain approximately 27,000.*

Fig. 15 shows how the total gas gain (i. e. the integral of multiplication and attachment processes) depends on the initial radial position of the primary electron. Electrons starting from the area close to the cathode pass through a region with an increased probability to be attached. Electrons from a conversion which are very close to the wire are not able to exploit the full multiplication path. This "competition" of Townsend and attachment coefficient leads to a maximum of multiplication that an electron can reach when it starts its life about 160 μm away from the wire (in case of no wire offset).

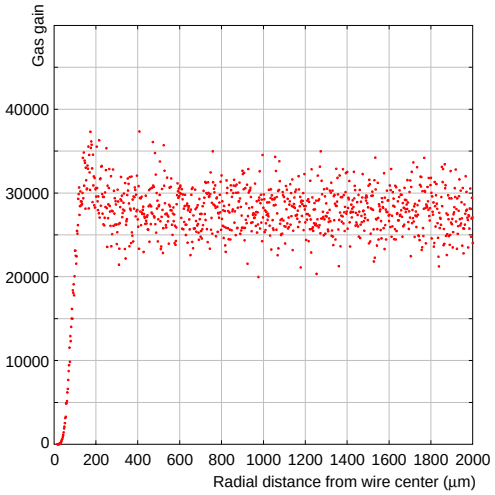

Figure 15: *Each point represents the Monte Carlo simulated multiplication factor of an ^{55}Fe cluster as a function of the initial drift distance from the wire (diameter 30 μm, 1530 V, no offset, TRT standard mixture)*

3.7 Effects of a wire offset

If the wire in the straw is displaced from the tube center the picture is changed. Electrons starting at the same distance from the wire but from different sides will generally not result in the same mean avalanche size. The gain dependency on the position of the deposited charge becomes worse. Fig. 16 shows straw areas which have the same (within 5%) gas gain for the case of 500 μm wire offset. The strongly varying signal pulses change the known Gaussian character of the distribution into a distribution with a higher probability for large avalanche

sizes. The effect becomes stronger with increasing wire offset (Fig. 17). In good approximation such a spectrum can be fitted with a double-Gaussian function (Fig. 18), which clearly can be related to a superposition of two spectra recorded from both sides, where the wire is closest and furthest from the tube wall.

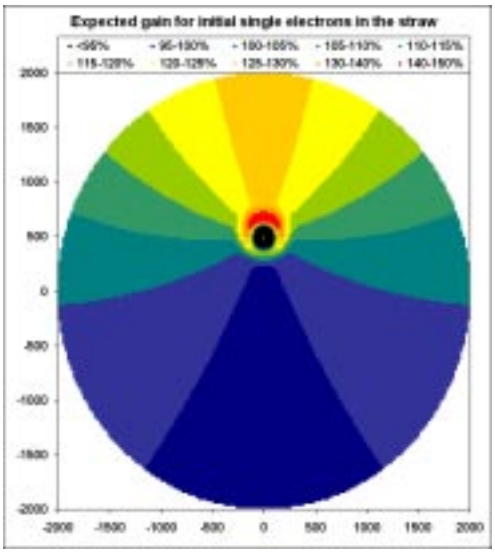

Figure 16: *Distribution of areas with similar gas gain in the straw with wire offset 500 μm. TRT standard mixture, 30 μm anode wire, 1530 V.*

The impact of a wire displacement on the straw operation was the main subject of interest in this work. Gas gain was simulated as a function of wire offset for our TRT standard gas mixture and a wire diameter of 30 μm. A comparison of the relative change in gas gain obtained in simulation and experiment is shown in Fig. 19. Good agreement for the wire offsets below 300 μm was found. The disagreement in the relative gain change for wire offsets above 300 μm is not completely understood yet, but may come from space charge effects in the locally high electric field region.

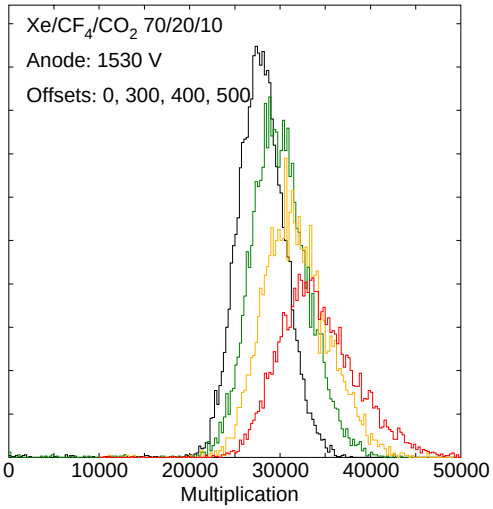

Figure 17: *Simulated spectra from point-like ionization of 5.9 keV for wire offsets of 0, 100, 300, 500 μm (from left to right). The energy resolutions are 21%, 23%, 26% and 27% respectively.*

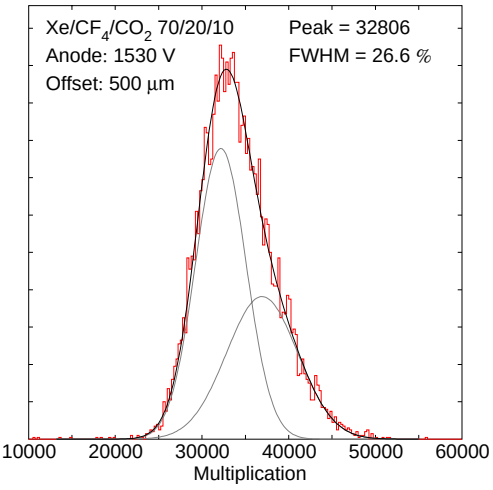

Figure 18: *Simulated spectrum fitted with a double-Gaussian function.*

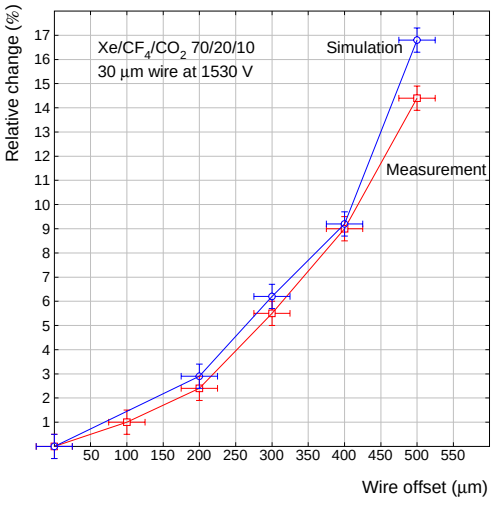

Figure 19: *Measured and simulated relative change in gas gain due to a wire offset in the straw.*

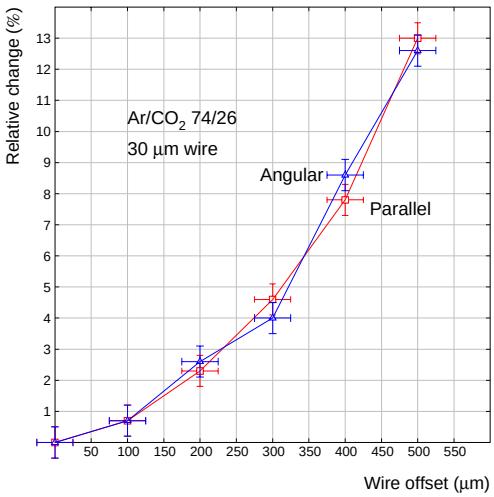

Figure 20: *Gas gain change as a function of wire displacement for Ar/CO_2 74/26 gas mixture. 30 µm wire diameter. Anode voltage of 1366 V. Parallel and angular wire displacement.*

4 Measurements in Argon based mixtures

It was already mentioned above that the main motivation of this work originated from practical issues, namely to understand the processes leading to a gas gain change when the wire moves out of the straw center and using this circumstance to specify calibration curves for wire offset measurements in all 425,000 straws of the ATLAS TRT. Xenon is an expensive gas and it might be important to use cheaper gas mixtures for testing purposes. Apart from the costs the main requirement on these mixtures is having operation properties as close as possible to the standard gas mixture (operating voltage, range of stable operation, robustness to discharges). For that reason different Ar-based mixtures have been examined.

Results of relative gas gain change versus wire offset for 30 μm wire fir Ar-based mixtures are shown in Figures 20 - 23.

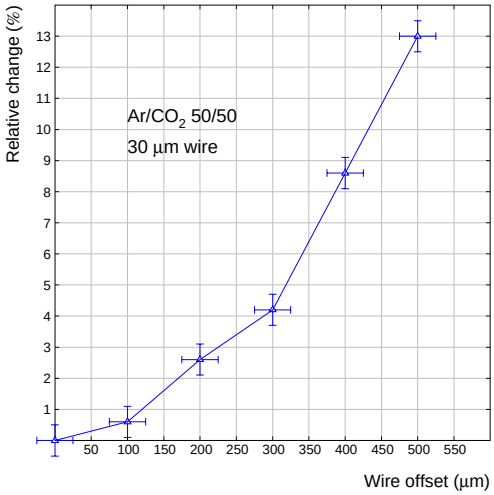

Figure 21: *Gas gain change as a function of wire displacement for Ar/CO_2 50/50 gas mixture. 30 µm wire diameter. Anode voltage of 1630 V. Angular wire displacement.*

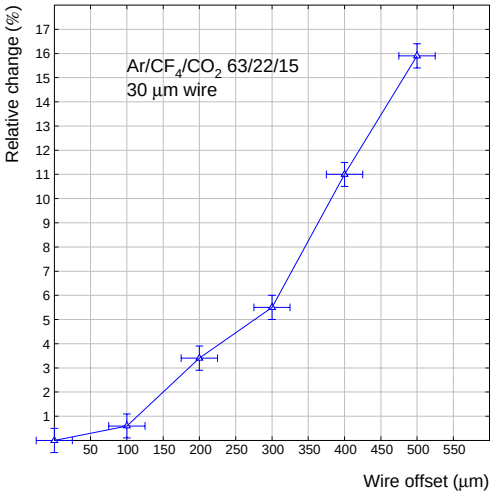

Figure 22: *Gas gain change as a function of wire displacement for $Ar/CF_4/CO_2$ 63/22/15 gas mixture. 30 μm wire diameter. Anode voltage of 1547 V. Angular wire displacement.*

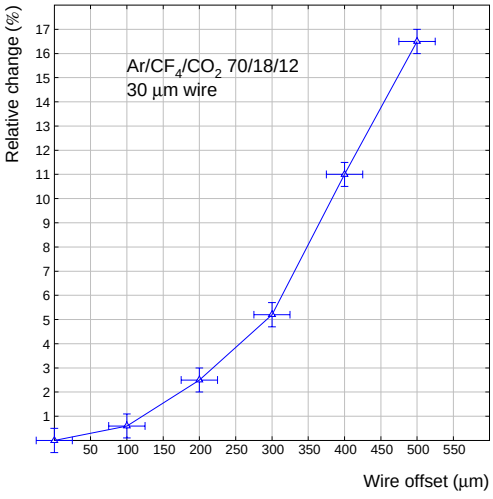

Figure 23: *Gas gain change as a function of wire displacement for $Ar/CF_4/CO_2$ 70/18/12 gas mixture. 30 μm wire diameter. Anode voltage of 1510 V. Angular wire displacement.*

One should not that there is no dependence on the beam orientation for Ar-based mixtures, (Fig. 20). That is because X-ray attenuation length in Argon is quite large and primary ionization clusters are distributed is the straw uniformity.

The sensitivity of the gas gain to a wire displacement is slightly higher for triple gas mixtures, what is important for wire offset measurement accuracy. $Ar/CF_4/CO_2$ 63/22/15 appeared to be the best choice, because its operating voltage and stability are very close to the TRT standard mixture. In contrary to that a two component mixture Ar/CO_2 74/26 needs less operating voltage (approximately by 200 V) and is not very resistant against discharges. In addition Ar/CO_2 mxiture is more sensitive to even small impurities of other gases particulary electronegative ones than triple mixture.

Ar/CO_2 50/50 requires a higher operating voltage but shows no improvement in operation stability. The data for 50 μm wires is shown in the Appendix.

5 Conclusion

It is shown that many properties of the straws can be well understood with the help of Monte Carlo studies. The simulations reproduce gain measurements within an acceptable error (of about 10%) in the allowed range of operation conditons. For larger gains, i. e. above 40,000, space-charge effects introduce non-linearities in the behavior and are not considered in the simulation. The relative change in gas gain due to a wire offset in the straw with the TRT gas mixture is well reproduced and understood.

One of the main achievement was

the success in obtaining the approximate width of the measured spectra. Even for no wire offset the energy resolution is limited through the large fraction of primary electrons attached in the gas, which leads to stronger fluctuations in the avalanche size. The increase of the FWHM with commencing wire offset becomes clear with the resulting field distortions. Only the improved avalanching model led to these results.

Electron transport properties have been computed with the help of *Magboltz* and were then used in *Garfield* to simulate drift and avalanching processes. The Monte Carlo integration has shown much better agreement than the analytic approach.

We have to emphasize that the only input in the Monte Carlo simulation are the various cross-sections of the gases, that come with the Magboltz code and are published data. No free parameters are used to "tune" the absolute multiplication values or the energy resolution in order to fit the experimental data. It shows that the underlying model of the straw behavior and properties is well understood.

As a result of the gas mixture studies it is shown that the wire offset can be measured using $Ar/CF_4/CO_2$ 63/22/15. This mixture behaves like the TRT standard Xenon mixture and has an enhanced sensitivity to wire offsets (3.5% and 5.6% for 200 μm and 300 μm offset respectively). A two component mixture of Argon and CO_2 does not look appropriate for these kind of studies, because of its insufficient stability against discharges and its lower sensitivity(2.5% and 4 % for 200 μm and 300 μm offset respectively). This difference is much larger for 50 μm wire diameter.

6 Acknowledgements

The authors would like to thank mainly Rob Veenhof, for his valuable contributions to this work and unconditional help. Also great thanks to Steve Biagi for providing his software and his profound knowledge.

A. Appendix

Measurements with 50 μm wires

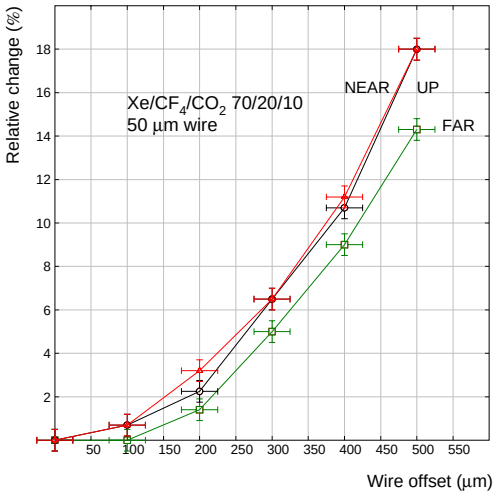

Figure 24: *Gas gain change as a function of the anode wire displacement for different directions of x-ray beam. TRT standard mixture, 50 μm wire diameter.*

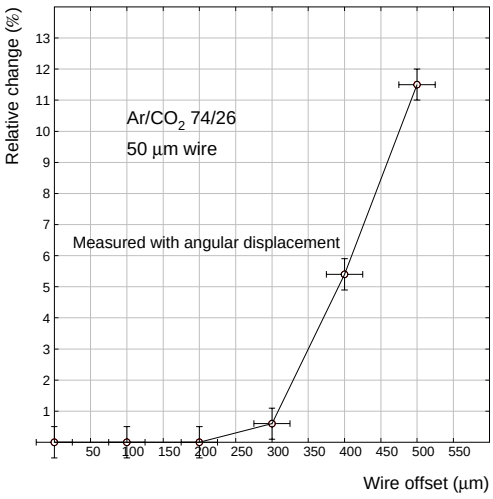

Figure 25: *Gas gain change as a function of wire displacement for Ar/CO_2 74/26 gas mixture. 50 μm wire diameter.*

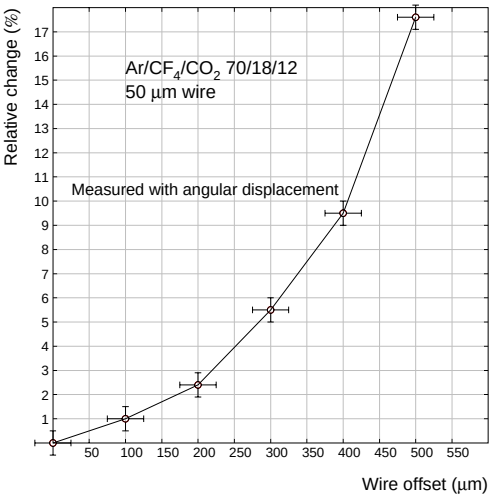

Figure 27: *Gas gain change as a function of wire displacement for $Ar/CF_4/CO_2$ 70/18/12 gas mixture 50 μm wire diameter.*

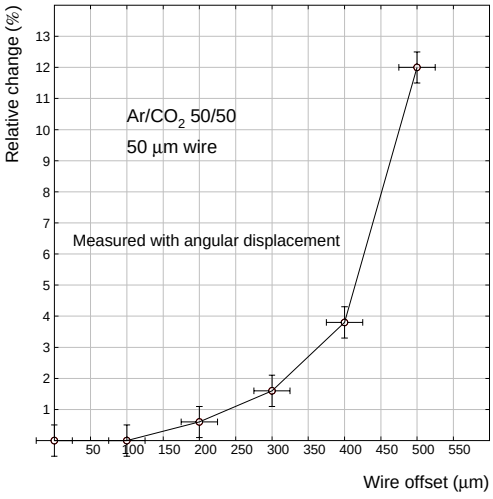

Figure 26: *Gas gain change as a function of wire displacement for Ar/CO_2 50/50 gas mixture. 50 μm wire diameter.*

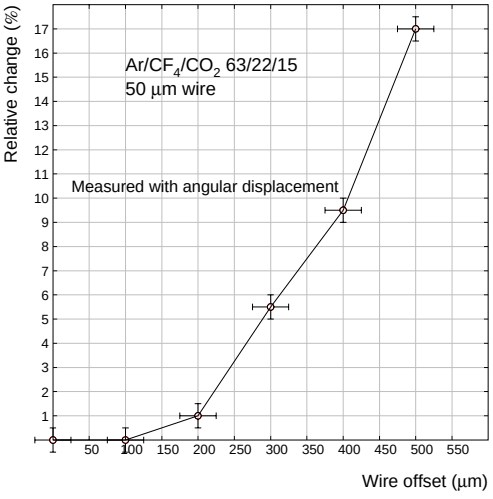

Figure 28: *Gas gain change as a function of wire displacement for $Ar/CF_4/CO_2$ 63/22/15 gas mixture 50 μm wire diameter.*

References

[1] ATLAS Collaboration, *ATLAS Inner Detector Technical Design Report*, CERN/LHCC/97-17, ATLAS TDR 5, 30 April 1997.

[2] W. S. Anderson et al., *Electron attachment, effective ionization coefficient and electron drift velocity for CF_4 gas mixtures.* Nucl. Instr. and Meth. A 323 (1992) 273-279

[3] B. Dolgoshein et al., *Gas Mixtures for Transition Radiation Detectors at High-Luminosity Colliders.* Nucl. Instr. and Meth. A 294 (1990) 473

[4] Rob Veenhof, *Garfield* - A drift chamber simulation program, CERN Program Library, 1998

[5] S. F. Biagi, *A Multiterm Boltzmann Analysis of Drift Velocity, Diffusion, Gain and Magnetic-field Effects in Argon-Methane-Water-Vapour Mixtures.* Nucl. Instr. and Meth. A 283 (1989) 716-722

[6] S. F. Biagi, *Monte Carlo simulation of electron drift and diffusion in counting gases under the influence of electric and magnetic fields.* Nucl. Instr. and Meth. A 421 (1999) 234-240

[7] recommended by Steve Biagi

[8] G. W. Fraser, E. Mathieson, Nucl. Instr. and Meth. A 247 (1986) 544

[9] Maxwell 2D Field Simulator, Ansoft Corporation.

[10] G. Charpak et al., Nucl. Instr. and Meth. A 148 (1978) 471-482;
H. vd Graaf, PhD thesis, TU Delft (1986);
T. J. Harris + E. Mathieson, Nucl. Instr. and Meth. A 154 (1978) 183-188, Nucl. Instr. and Meth. A 159 (1979) 483-487;

[11] W. Legler, *Zur Statistik der Elektronenlawinen.* Z. Phys., 140, 221 [1955]

[12] W. Legler, *Die Statistik der Elektronenlawinen in elektronegativen Gasen, bei hohen Feldstärken und bei großer Gasverstärkung.* Z. Naturforschg. 16a, 253-261 [1961]

[13] private communication with Rob Veenhof

[14] private communication with Steve Biagi

[15] U. Fano, Phys. Rev. 72 26-9